Reviving the energy independent suppression of the solar neutrino flux

Sandhya Choubey,[1] Srubabati Goswami,[1] Nayantara Gupta,[2] and D. P. Roy[3]
[1]*Saha Institute of Nuclear Physics, 1/AF, Bidhannagar, Calcutta 700 064, India*
[2]*Indian Association for the Cultivation of Sciences, Calcutta 700 032, India*
[3]*Tata Institute of Fundamental Research, Homi Bhabha Road, Mumbai 400 005, India*
(Received 12 April 2001; published 19 July 2001)

We explore the possibility of an energy independent suppression of the solar neutrino flux in the context of the recent SuperKamiokande data. From a global analysis of the rate and spectrum data, this scenario is allowed at only 14% probability with the observed Cl rate. If we allow for a 20% upward renormalization of the Cl rate along with a downward renormalization of the *B* neutrino flux then the fit improves considerably to a probability of $\sim 50\%$. We compare the quality of these fits with those of the MSW solutions. These renormalizations are also found to improve the quality of the fits with MSW solutions and enlarge the allowed region of their validity in the parameter space substantially. Over much of this enlarged region the matter effects on the suppression of the solar neutrino flux are found to be very weak, so that the solutions become practically energy independent.

DOI: 10.1103/PhysRevD.64.053002 PACS number(s): 14.60.Pq, 13.35.Hb, 26.65.+t, 96.40.Tv

The results from the SuperKamiokande (SK) continue to confirm the suppression of the solar neutrino flux as compared to the standard solar model prediction [1]. The result from the GNO experiment [2] is consistent with the earlier Ga experiment results from GALLEX and SAGE [3]. The most popular explanation for this suppression is neutrino oscillation either in vacuum or in matter. Table I shows the suppression rate or survival probability of the solar neutrino ($P_{\nu_e\nu_e}$) from the combined Ga [2,3], Cl [4] and SK [1] experiments along with their energy thresholds. The corresponding compositions of the solar neutrino flux are also indicated. The SK suppression rate shown in brackets is appropriate for the oscillation of ν_e into another active neutrino ($\nu_{\mu,\tau}$). It is obtained by subtracting the neutral current contribution of $\nu_{\mu,\tau}$ from the SK rate.

The observed energy dependence in the suppression rates in Ga, Cl and SK experiments can be explained by the vacuum oscillation (VO), small and large mixing angle (SMA and LMA) Mikheyev-Smirnov-Wolfenstein (MSW) as well as the low probability, low mass (LOW) solutions [5]. The apparent energy dependence comes from assuming the Sun-Earth distance to coincide with the oscillation node of a MeV range neutrino in the VO solution, while it comes from matter effects in the sun for the MSW solutions and in the Earth for the LOW solution. The VO and SMA solutions show a strong and nonmonotonic energy dependence. But the LMA and LOW solutions show a monotonic decrease from Ga to SK energies in contrast with the apparent rise between the Cl and SK rates.

The recent SK data on the energy spectra at day and night show no evidence of any energy dependence nor any day-night asymmetry in the suppression rate [1]. This rules out a large part of the parameter space. In particular it practically rules out the VO solution and disfavors the SMA along with a part of the LMA solution [1,6]. The remaining part of the LMA solution and the low solution show relatively weak energy dependence and cover two small patches in the parameter space. Thus it is possible to explain the above mentioned rates and the energy spectra only for very limited ranges of neutrino mass Δm^2 and mixing angle θ.

We present here fits to the above data, first with an energy independent solution and then with two-flavor oscillation including matter effects. We shall see that with reasonable allowance for the renormalizations of the Cl rate and the *B* neutrino flux the data are described well by the energy independent solution. These renormalizations shall also be seen to improve the quality of fits with the oscillation solutions and enlarge the region of their validity in the parameter space substantially. Moreover we shall see that most of this enlarged region of parameter space shows weak matter effect on $P_{\nu_e\nu_e}$, implying practically energy independent suppression of the solar neutrino flux. Thus the energy independent solution can be looked upon as an effective parametrization of the oscillation solutions over this region.

The definition of χ^2 used in our fits is

$$\chi^2 = \sum_{i,j} (F_i^{th} - F_i^{exp})(\sigma_{ij}^{-2})(F_j^{th} - F_j^{exp}) \qquad (1)$$

where i,j runs over the number of experimental data points. Here $F_i^{\alpha} = T_i^{\alpha}/T_i^{BP00}$ where α is the theoretical prediction or the experimental value of the event rate, normalized by the standard solar model prediction of Bahcall, Pinsonneault, and Basu (BPB00) [7]. F_i^{exp} is taken from Table I for total rates and from [8] for day-night spectrum. The error matrix σ_{ij} contains the experimental errors, the theoretical errors and their correlations. For evaluating the error matrix we use the procedure described in [9]. The details of the solar neutrino code used is described in [10,11]. As in [12] we vary the normalization of the spectrum as a free parameter which avoids the overcounting of the rates and spectrum data for SK. Hence for the day-night spectrum analysis we have (36 - 1) degrees of freedom (DOF) while for the total rates we have 3, which makes a total of 38 DOF for the rates +spectrum analysis. In addition to the best-fit parameter values and χ^2_{min} we shall present the goodness of fit (GOF) of a solution where by GOF we mean the probability that the χ^2 will exceed the χ^2_{min} for a correct model. Finally for the general oscillation solution with matter effects, we shall also

TABLE I. The suppression rates of solar neutrino $P_{\nu_e\nu_e}$ shown for Ga, Cl and SK experiments [1–6] along with their threshold energies and compositions. The effective suppression rate of the SK experiment, appropriate for $\nu_e \to \nu_{\mu,\tau}$ oscillation, is shown in parentheses. All the suppression rates are shown relative to the standard solar model prediction of BPB00 [7].

Experiment	Gallium	Chlorine	SuperKamiokande
Suppr. Rate	0.576 ± 0.04	0.327 ± 0.029	0.465 ± 0.015 ($0.36 \pm .015$)
E_{th} (MeV)	0.2	0.8	6.5
Composition	pp(55%), Be (25%), B (10%)	B (75%), Be (15%)	B (100%)

delineate the 90%, 95% and 99% allowed regions in the two parameter $\Delta m^2 - \tan^2\theta$ plane. These regions are defined as $\chi^2 \leqslant \chi^2_{min} + \Delta\chi^2$ where $\Delta\chi^2$ is 4.61,5.99,9.21 respectively for two parameters and the χ^2_{min} corresponds to the global χ^2 minimum [13].

ENERGY INDEPENDENT SOLUTION

We shall explore first the possibility of explaining these data in terms of a simple energy independent solution by assuming modest changes in the Cl rate and the *B* neutrino flux. Energy independent solutions to the solar neutrino anomaly have been considered by several authors in the past [14]. Traditionally it is associated with the vacuum oscillation solution at a distance much larger than the oscillation wavelength, so that the average survival probability

$$P_{\nu_e\nu_e} = 1 - \frac{1}{2}\sin^2 2\theta. \tag{2}$$

We shall see below however that this survival probability remains approximately valid over a wide range of parameters even after including the matter effects in the Sun and the Earth, since the matter effects over this range are too small to be measurable at the present level of experimental accuracy. In particular the so called bimaximal mixing solution, corresponding to nearly maximal mixing of solar neutrino (ν_e), implies such an energy independent solution over a very wide range of Δm^2 [15]. Moreover an energy independent solution to the solar neutrino anomaly seems to offer the possibility of explaining the atmospheric and the LSND neutrino anomalies as well without assuming any sterile neutrino [16].

We present the results of our fit to the combined data on rates and the SK day-night spectrum with the energy independent solution (2) in Table II for both ν_e oscillations into active and sterile neutrinos. In order to reconcile the energy independence of the spectrum with the apparent energy dependence in the rates of Table I, we have considered the following changes in the Cl rate and *B* neutrino flux.

(A) Chlorine Rate: Since the Cl experiment [4] has not been calibrated, there are several fits in the literature disregarding this rate [6,17,18]. In any case the apparent rise between the Cl and SK rates is in direct conflict with the predicted fall for the LMA and LOW solutions, which are favored by the spectrum data. Therefore we have considered an upward renormalization of the Cl data by 20%, which is a 2σ effect.

(B) Boron Neutrino Flux: The *B* neutrino flux is very sensitive to the solar core temperature and hence to the underlying solar model. Even within the standard solar model estimate of BPB00 it has a large error bar, i.e.

$$f_B = 5.15 \times 10^6 \ \text{cm}^{-2} \ \text{sec}^{-1} \begin{pmatrix} & +.20 \\ 1.0 & \\ & -.16 \end{pmatrix}. \tag{3}$$

Therefore we have considered a variation of this flux within a corridor of about $\pm 2\sigma$ of the above central value.

Table II shows that taking the experimental rates at their face value results in a poor fit to the energy independent solution, corresponding to a probability of 14.39 (3.75)% for the active (sterile) case. But assuming a 20% renormalization of the Cl rate and floating the normalization of *B* flux improves the probability to 46.6 (26.4)%. Let us comment on two related features of this fit, which may appear counterintuitive. The theoretical survival rate from Eq. (2) is $\geqslant 0.5$ while the experimental rates from Cl and SK with the BPB00 *B* neutrino flux are significantly lower than 0.5 (Table I).

TABLE II. The best-fit value of the parameter, the χ^2_{min} and the GOF from a combined analysis of rate and spectrum with the energy independent solution (2).

	Nature of solution	X_B	$\sin^2 2\theta \begin{pmatrix} \tan^2\theta \\ \text{or} \\ \cot^2\theta \end{pmatrix}$	χ^2_{min}	Goodness of fit
Chlorine observed	Active	1.0	0.95(0.63)	46.15	14.39%
		0.77	0.96(0.68)	45.86	12.25%
	Sterile	1.0	0.89(0.52)	53.66	3.75%
		0.83	0.92(0.57)	54.63	2.55%
Chlorine renormalized	Active	1.0	0.89(0.52)	37.65	43.13%
		0.73	0.88(0.50)	36.05	46.63%
	Sterile	1.0	0.85(0.44)	40.89	30.35%
		0.79	0.85(0.44)	40.09	26.4%

Thus one would naively expect the fit with the BPB00 neutrino flux, denoted by $X_B=1$, to result in $\sin^2 2\theta=1$ and a much larger χ^2_{min} than the free X_B fit. We have checked these to be true if we drop the theoretical error in Eq. (1), reducing it to the standard expression for χ^2. However including the large uncertainty in the B neutrino flux of Eq. (3) via the theoretical error matrix implies that the best fit with the BPB00 flux ($X_B=1$ solution) corresponds actually to an X_B significantly lower than 1. Hence the corresponding χ^2_{min} and $\sin^2 2\theta$ values are close to those of the free X_B fit. The χ^2_{min} is found to be quite flat in $\sin^2 2\theta$ (and even more so in $\tan^2\theta$) in the region around the best-fit values. It may be noted here that using 1σ lower limits of the appropriate nuclear reaction rates Brun, Truck-Chieze and Morel [19] have obtained a relatively low value of B neutrino flux,

$$f_B = 3.21\times 10^6 \ \ \mathrm{cm}^{-2} \ \ \mathrm{sec}^{-1}, \tag{4}$$

and found it to give better agreement to the helioseismic data than Eq. (3). This corresponds to a low value of $X_B \simeq 0.63$, which is about 2σ below the central value of Eq. (3). More recently a $X_B \simeq 0.75$ has been obtained from the helioseismic model using standard values of the nuclear reaction rates [20].

OSCILLATION SOLUTION WITH MATTER EFFECTS

We shall first analyze the two-flavor oscillation solution, including the matter effects in the sun and the earth, to determine the region of the $\Delta m^2-\tan^2\theta$ plane in which it effectively reduces to the energy independent solution (2). Since the normalization uncertainty of Ga and Cl experiments are $>10\%$ each, one cannot experimentally distinguish the solutions showing energy dependence of $<10\%$ over the energy range of Ga to SK experimeriments from the energy independent solution (2). We have therefore assumed that a matter effect of $<10\%$ on $P_{\nu_e\nu_e}$ over the range of Ga to SK neutrino energies is a good working definition for an effectively energy independent solution (2). Figure 1 shows the region in the $\Delta m^2-\tan^2\theta$ plane, where the oscillation solution including matter effects effectively reduces to the energy independent solution (2). We have restricted the plot to $\Delta m^2 < 10^{-3}$ eV^2 in view of the severe constraint from the CHOOZ experiment above this range [21]. One sees from Fig. 1 two distinct regions of validity of the energy independent solution (2). Firstly the solar matter effect is negligible in the shaded region above the MSW range [17]

$$10^{-15} \ \ \mathrm{eV} \lesssim \Delta m^2/4E \lesssim 10^{-11} \ \ \mathrm{eV}, \tag{5}$$

with $4E \sim 1-50$ MeV, along with the triangular region below. Moreover a narrow strip around $\tan^2\theta=1$ represents the region of near maximal-mixing, where the MSW solution for $P_{\nu_e\nu_e}$ reduces to the vacuum solution (2). However the regeneration effect in earth makes a significant contribution to the maximal-mixing region over $\Delta m^2 \simeq 10^{-5}-10^{-7}$ eV^2, which accounts for the gap in this strip. It is this near maximal-mixing strip that is relevant for the energy independent solution of Table II and the oscillation solutions presented below.

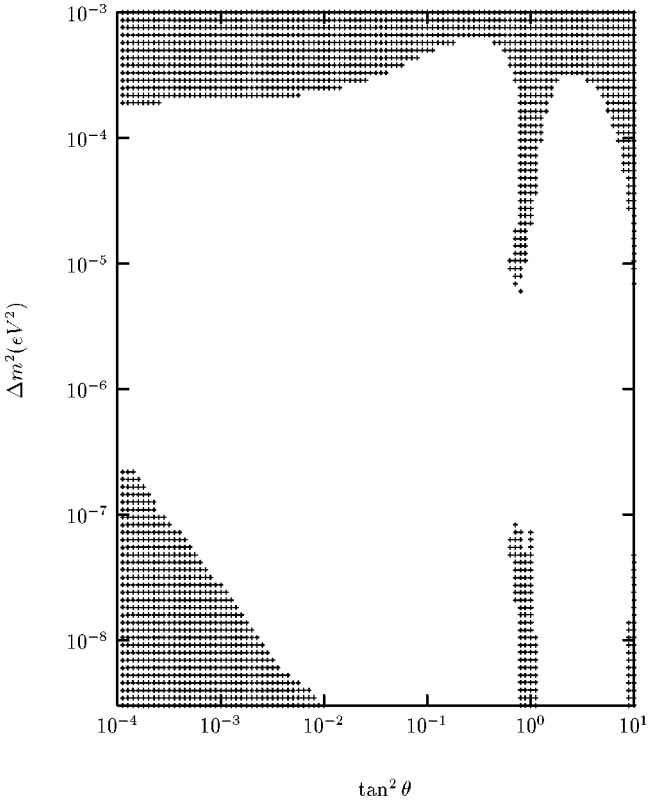

FIG. 1. The quasi-energy-independent allowed region in $\Delta m^2-\tan^2\theta$ parameter space where the solar neutrino survival probability agrees with Eq. (2) to within 10% over the Ga and SK energies.

We shall now present the fits of the oscillation solutions including matter effects to the combined data on rates and the SK day-night spectrum. As in the previous case we have done these fits with the rates shown in Table I as well as those with renormalized Cl rate and B neutrino flux.

Table III summarizes the results of fitting the oscillation solutions to the combined data with the observed and renormalized Cl rates assuming the B neutrino flux of BPB00 ($X_B=1$). We see from the upper part of this table that one can get acceptable fits to the data taken at its face value in terms of ν_e oscillation into active flavor in the LMA and LOW regions, while the SMA region gives a marginal fit at 19% probability. The corresponding oscillation solutions into sterile neutrino give poor fits. Renormalizing the Cl rate upwards by 20% improves the quality of oscillation solutions into active flavor remarkably in the LMA and LOW regions but not in the SMA region. The quality of the sterile solutions also improves to acceptable levels of probability; but they remain inferior to the oscillation solutions into active neutrino.

A clear pedagogical discussion of the LMA and LOW solutions can be found in [17]. We shall only point out here some essential features, focussing on the oscillation into active neutrino. The Δm^2 of the LMA solutions of Table III lie at the upper edge (adiabatic edge) of the MSW range (5). They lie outside this range for Ga energy, so that the corre-

TABLE III. The best-fit values of the parameters, the $\chi^2_{\rm min}$ and the GOF from a combined analysis of rate and spectrum in terms of ν_e oscillation into an active-sterile neutrino, including the matter effects.

	Type of neutrino	Nature of solution	Δm^2 in eV^2	$\tan^2\theta$	χ^2_{min}	GOF
		SMA	5.48×10^{-6}	5.79×10^{-4}	43.22	19.01%
	Active	LMA	4.18×10^{-5}	0.36	37.33	40.78%
Cl		LOW	1.51×10^{-7}	0.64	39.54	31.48%
obsvd.		SMA	3.74×10^{-6}	5.2×10^{-4}	44.85	14.79%
	Sterile	LMA	1.03×10^{-4}	0.58	52.18	3.96%
		LOW	3.47×10^{-8}	0.82	50.57	5.43%
		SMA	4.97×10^{-6}	3.15×10^{-4}	42.43	21.37%
Cl	Active	LMA	6.68×10^{-5}	0.39	30.32	73.53%
renorm.		LOW	1.63×10^{-7}	0.76	32.43	63.9%
		SMA	3.44×10^{-6}	3.59×10^{-4}	41.98	22.76%
	Sterile	LMA	1.04×10^{-4}	0.53	37.9	38.27%
		LOW	4.08×10^{-8}	0.84	36.8	42.98%

sponding survival rate is approximated by Eq. (2), or equivalently

$$P_{\nu_e\nu_e}\approx\frac{1}{2}(1+\epsilon^2), \tag{6}$$

$$\epsilon=\cos 2\theta=\frac{1-\tan^2\theta}{1+\tan^2\theta}. \tag{7}$$

On the other hand, they lie inside the MSW range at SK energy. Here the solar ν_e gets adiabatically converted into the heavier one of the two neutrino mass states,

$$\nu_2=\sin\theta\cdot\nu_e+\cos\theta\cdot\nu_{\mu,\tau}. \tag{8}$$

The resulting survival probability on earth is

$$P_{\nu_e\nu_e}\approx\sin^2\theta=\frac{1}{2}(1-\epsilon). \tag{9}$$

With the LMA mixing angles of Table III, corresponding to $\epsilon\simeq0.4$, Eqs. (6) and (9) can be seen to roughly reproduce the Ga and SK rates of Table I. In the LOW solutions the energy dependence arises from the ν_e regeneration in earth during the night. This is known to be small for the SK energy from the absence of day-night asymmetry, so that the corresponding rate (9) is valid for the LOW solution as well. However the regeneration contribution can be significant for the LOW solution at Ga energy, which has moved into the MSW range (5). The corresponding rate after averaging over day and night is [17]

$$\overline{P}_{\nu_e\nu_e}=\frac{1}{2}(1-\epsilon+f_{reg}). \tag{10}$$

For a constant density Earth,

$$f_{reg}=\frac{\eta_E(1-\epsilon^2)}{2(1-2\epsilon\eta_E+\eta_E^2)}. \tag{11}$$

Thus the earth regeneration contribution is always positive and can be significant for $\eta_E\sim1$, where

$$\eta_E=0.66\left(\frac{\Delta m^2/E}{10^{-13}\ \text{eV}}\right)\left(\frac{g/\text{cm}^3}{\rho Y_e}\right). \tag{12}$$

Here ρ is the matter density in earth and Y_e the average number of electrons per nucleon. The maximal contribution comes from $\Delta m^2\sim3E\times10^{-13}$ eV-10^{-7} eV^2 for Ga energy. The mixing angle of the LOW solutions, $\epsilon\sim0.2$, corresponds to a maximal $f_{reg}\sim0.3$, which can account for the Ga rate of Table I. While this description of the matter effects in the Sun and the Earth is admittedly simplistic we have treated them rigorously in our calculation at all energies.

Figure 2 shows the 90%, 95% and 99% C.L. allowed regions in the $\Delta m^2-\tan^2\theta$ plane for the oscillation solutions into active neutrino. We find that SMA solution is disallowed at 95% (99%) C.L. with the observed (renormalized) Cl rate. The allowed regions of the LMA and LOW solutions increase mildly with the upward renormalization of the Cl rate. Comparison of Figs. 1 and 2 shows that modest parts of the allowed regions for both the LMA and LOW solutions correspond to the effectively energy independent solution (2).

Table IV summarizes the effects of changing the B neutrino flux (X_B) on the oscillations solutions into active neutrino. It lists the best solutions for $X_B=0.75$, favored by helioseismic model [20], as well as for free X_B. In each case the solutions are shown for both observed and renormalized Cl rates. It may be noted that the $X_B=0.75$ lies within $\sim1.5\sigma$ of the BPB00 flux (3). In combination with the 20% renormalization of the Cl rate it would imply that all the suppression rates of Table I agree with one another within 1.5σ. Therefore this combination is expected to favor an effectively energy independent solution.

As we see from the top part of Table IV, with observed Cl rate and $X_B=0.75$ the SMA gives a better fit than the LMA and LOW solutions. This is because reducing X_B to 0.75 accentuates the rise between the Cl and the SK rates of Table I as it enhances the latter by a larger amount. Hence it favors the nonmonotonic energy dependence of SMA over the monotonically decreasing energy dependence of LMA and

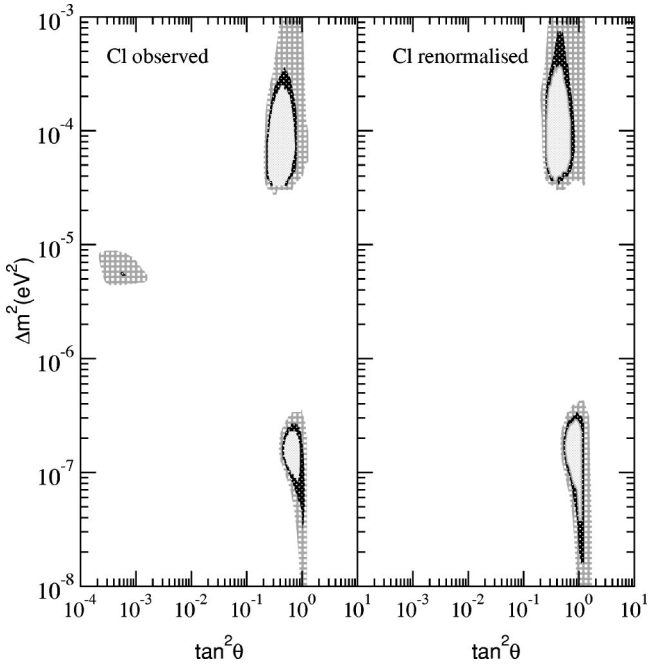

FIG. 2. The 90, 95 and 99% C.L. allowed area from the global analysis of the total rates from Cl (observed and 20% renormalized), Ga and SK detectors and the 1117 days SK recoil electron spectrum at day and night, assuming MSW conversions to active neutrinos.

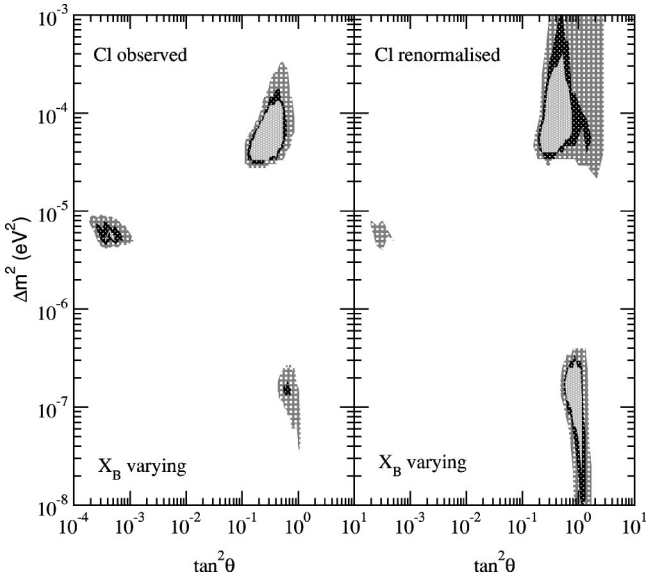

FIG. 3. The 90, 95 and 99% C.L. allowed area from the global analysis of the total rates from Cl (observed and 20% renormalized), Ga and SK detectors and the 1117 days SK recoil electron spectrum at day and night, assuming MSW conversions to active neutrinos. The B normalization is floated as a free parameter.

LOW solutions. However this anomaly disappears with the upward renormalization of the Cl rate, so that the LMA and LOW solutions become much better than the SMA. Note also that reducing X_B to 0.75 results in reducing the energy dependence between the Ga and SK rates, resulting in larger mixing angle for the LMA solutions than in Table III.

The free X_B fits yield $X_B=0.5-0.6$ for the SMA and $X_B>1$ for the LMA solutions. This is because $X_B=0.5-0.6$ enhances the SK rate more than Cl as favored by SMA, while $X_B>1$ suppresses the SK rate more than Cl as favored by the LMA solutions. Note however that $X_B>1$ magnifies the decrease between the Ga and SK rates, resulting in a smaller mixing angle for the LMA solutions than in Table III. But the shift is small for the renormalized Cl rate. The LOW solution gives the worst fit for the observed Cl rate, since its weak energy dependene favors $X_B<1$ which accentuates the rise between the Cl and SK rates. But with renormalized Cl the LMA and LOW solutions become much better than the SMA.

Figure 3 shows the 90%, 95% and 99% C.L. allowed regions in the $\Delta m^2-\tan^2\theta$ plane for the free X_B fits. With the observed Cl rate the LMA region covers relatively small mixing angles while the LOW region is marginal. Consequently there is little overlap with the energy independent region of Fig. 1. However for the renormalized Cl rate the LMA region expands to larger mixing angles and masses. The LOW region also covers a large range of mass. Conse-

TABLE IV. Best fits to the combined rates and spectrum data in terms of ν_e oscillation into active neutrino with $X_B=0.75$ and free X_B.

		Nature of Solution	Δm^2 in eV^2	$\tan^2\theta$	χ^2_{min}	GOF
		SMA	5.43×10^{-6}	5.09×10^{-4}	39.50	31.64%
	$X_B=0.75$	LMA	4.39×10^{-5}	0.54	43.18	19.13%
Cl		LOW	1.41×10^{-7}	0.69	41.88	23.08%
obsvd.	0.57	SMA	5.35×10^{-6}	4.35×10^{-4}	37.98	37.92%
	X_B 1.34	LMA	4.21×10^{-5}	0.25	34.22	55.34%
	0.93	LOW	1.51×10^{-7}	0.63	39.59	31.28%
		SMA	4.95×10^{-6}	3.11×10^{-4}	38.15	37.19%
Cl	$X_B=0.75$	LMA	6.92×10^{-5}	0.57	34.06	56.11%
renorm.		LOW	1.59×10^{-7}	0.82	32.76	62.35%
	0.53	SMA	4.90×10^{-6}	2.92×10^{-4}	35.57	48.89%
	X_B 1.14	LMA	6.57×10^{-5}	0.35	29.94	75.14%
	0.88	LOW	1.64×10^{-7}	0.76	31.95	66.17%

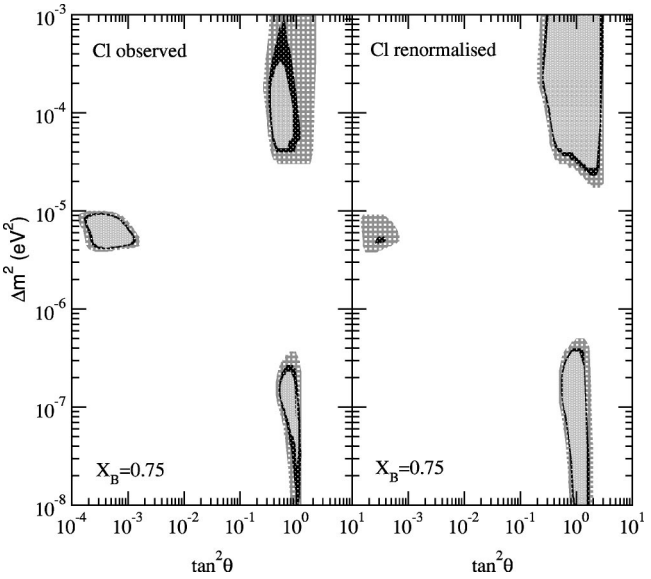

FIG. 4. The 90, 95 and 99% C.L. allowed area from the global analysis of the total rates from Cl (observed and 20% renormalized), Ga and SK detectors and the 1117 days SK recoil electron spectrum at day and night, assuming MSW conversions to active neutrinos. The B normalization is held fixed at 0.75 of SSM value.

quently there is a significant overlap with the energy independent region of Fig. 1.

Finally Fig. 4 shows the corresponding allowed regions for $X_B=0.75$ fits with observed and renormalized Cl rates. In the former case there is a large allowed region at 90% C.L. for the SMA solution. However in the latter case the 90% C.L. region disappears from the SMA solution, while covering a very large range of masses and mixing angles for the LMA and LOW solutions. Comparing this contour with Fig. 1 shows that the bulk of the expanded 90% C.L. region in this case corresponds effectively to the energy independent suppresion rate (2), as anticipated earlier. Note in particular the expansion of the 90% C.L. allowed region of the LMA solution well into the so called dark region, corresponding to $\tan^2\theta>1$ $(\epsilon<0)$. In this region the MSW prediction of energy dependence via Eqs. (6),(9) changes its direction, which goes against the direction of the data. Nonetheless the energy dependence becomes so mild with $X_B=0.75$ that the 90% C.L. region extends upto $\tan^2\theta>2$, which is beyond the range shown in Fig. 1. In other words the region of effectively energy independent solution shown in Fig. 1 is a conservative one. The expansion of the 90% C.L. region of the LOW solution also shows remarkable overlap with the lower energy independent strip of Fig. 1. It may be added here that both these strips go down to $\Delta m^2\sim 10^{-9}$ eV^2, below which one gets significant energy dependence from vacuum oscillation.

Let us conclude by briefly discussing whether some of the forthcoming neutrino experiments will be able to discriminate between the energy independent and the MSW solutions. In particular the SNO experiment [22] is expected to provide both the charged current and neutral current scattering rates over roughly the same energy range as SK. Thus the *B* neutrino flux can be factored out from their ratio, CC/NC.

TABLE V. The R_{cc}/R_{nc} at SNO at the best-fit values for the LMA, LOW and energy independent solution for the renormalized chlorine and X_B fixed cases of Table II and Table III.

Nature of solution	Δm^2	$\tan^2\theta$	R_{cc}/R_{nc}
LMA	6.68×10^{-5}	0.39	0.32
LOW	1.63×10^{-7}	0.76	0.45
energy independent	-	0.52	0.55

For oscillation into active neutrino this ratio is predicted to be larger than 0.5 for the energy independent solution [Eq. (2)] and smaller than 0.5 for the LMA and LOW solutions [Eq. (9)]. We have calculated the best fit values of this ratio for the energy independent solution of Table II and the LMA and LOW solutions of Table III with renormalized Cl rate. The predicted ratios are shown in Table V. With a sample of 5000 CC and 2000 NC events the total 1σ error for this ratio at SNO is expected to be about 4% [17]. This will be able to distinguish the energy idependent solution clearly from the LMA and to a lesser extent from the LOW solution. On the other hand, the LOW solution predicts a large day-night asymmetry of $>10\%$ for the Be neutrino [17,18] at the Borexino [23] and the KamLAND [24] experiments. This will be able to distingusish the LOW from the LMA and the energy independent solutions. Lastly it should be noted that the reactor neutrino data at KamLAND is expected to show oscillatory behavior for the LMA solution [25], which will help to distinguish it from the LOW or a generic energy independent solution.

SUMMARY

In summary the recent SK data on day-night spectrum is in potential conflict with the apparent energy dependence in the suppression rates observed in Ga, Cl and SK experiments. Including matter effects one can get acceptable oscillation solutions to both rates and spectrum data only over limited regions of mass and mixing parameters. However an upward renormalization of the Cl rate by 20% (2σ) results in substantial improvement of the quality of fit. Moreover a downward renormalization of the *B* neutrino flux by 25% (1.5σ) as suggested by the helioseismic model enlarges the allowed region of the parameter space substantially. Over most of this enlarged region the energy dependence resulting from the matter effects is too weak to be discernible at the present level of experimental accuracy. Hence with these renormalizations of the Cl rate and the *B* neutrino flux the data can be described very well by an energy independent solution.

Note added. After this work was completed the 1258 days SK data has appeared on the net [26]. We have checked that the results of our analysis do not show any significant changes with the new data.

We thank Professor H. M. Antia, Professor G. Bhattacharya, Professor S. M. Chitre, Professor K. Kar, and Professor A. Raychaudhuri for discussions.

[1] SK Collaboration, Y. Suzuki, in Neutrino 200, Sudbury, Canada (2000); the results of all the neutrino experiments presented at the Neutrino2000 meeting can be found at http://nu2000.sno.laurentian.ca.
[2] M. Altmann *et al.*, Phys. Lett. B **490**, 16 (2000).
[3] The GALLEX Collaboration, W. Hampel *et al.*, Phys. Lett. B **388**, 384 (1996); The SAGE Collaboration, J. N. Abdurashitov *et al.*, Phys. Rev. Lett. **77**, 4708 (1996).
[4] B. T. Cleveland *et al.*, Astrophys. J. **496**, 505 (1998); R. Davis, Prog. Part. Nucl. Phys. **32**, 13 (1994).
[5] J. N. Bahcall, P. I. Kraslev, and A. Y. Smirnov, Phys. Rev. D **58**, 096016 (1998).
[6] M. C. Gonzalez-Garcia, C. Peña-Garay, Nucl. Phys. B (Proc. Suppl.) **91**, 80 (2000).
[7] J. N. Bahcall, M. H. Pinsonneault, and Sarbani Basu, astro-ph/0010346.
[8] The day-night spectrum data used are obtained from the SK Collaboration, Y. Suzuki (private communication).
[9] G. L. Fogli and E. Lisi, Astropart. Phys. **3**, 185 (1995).
[10] S. Goswami, D. Majumdar, and A. Raychaudhuri, hep-ph/9909453; Phys. Rev. D **63**, 013003 (2001).
[11] A. Bandyopadhyay, S. Choubey, and S. Goswami, Phys. Rev. D **63**, 113019 (2001).
[12] M. C. Gonzalez-Garcia, P. C. de Holanda, C. Peña-Garay, and J. W. F. Valle, Nucl. Phys. **B573**, 3 (2000).
[13] See, e.g., W. Press *et al.*, *Numerical Recipe in Fortran 77*, 2nd ed. (Cambridge University Press, Cambridge, England, 1991).
[14] A. Acker, S. Pakvasa, J. Learned, and T. J. Weiler, Phys. Lett. B **298**, 149 (1993); P. F. Harrison, D. H. Perkins, and W. G. Scott, *ibid.* **349**, 137 (1995); **374**, 111 (1996); R. Foot and R. R. Volkas, hep-ph/9510312; A. Acker and S. Pakvasa, Phys. Lett. B **397**, 209 (1997); P. I. Krastev and S. T. Petkov, *ibid.* **395**, 69 (1997); G. Conforto *et al.*, *ibid.* **427**, 314 (1998); W. G. Scott, Nucl. Phys. B (Proc. Suppl.) **66**, 411 (1998) and hep-ph/0010335.
[15] Y. Grossman and Y. Nir, Nucl. Phys. **B448**, 30 (1995); R. Barbieri, L. Hall, D. Smith, A. Strumia, and N. Weiner, J. High Energy Phys. **12**, 017 (1998).
[16] G. Barenboim and F. Scheck, Phys. Lett. B **440**, 332 (1998).
[17] M. C. Gonzalez-Garcia, C. Pena-Garay, Y. Nir, and A. Yu. Smirnov, Phys. Rev. D **63**, 013007 (2001).
[18] Andre de Gouvea, A. Friedland, and H. Murayama, Phys. Lett. B **490**, 125 (2000).
[19] A. S. Brun, S. Truck-Chize, and P. Morel, Astrophys. J. **506**, 913 (1998).
[20] H. M. Antia and S. M. Chitre, Astron. Astrophys. **347**, 1000 (1999); S. Goswami, K. Kar, H. M. Antia, and S. M. Chitre, in Proceedings of the Helio and Asteroseismology at the Dawn of the Millennium, Tenerife, Spain, 2000 (in press).
[21] M. Apollonio *et al.*, Phys. Lett. B **446**, 415 (1999).
[22] SNO Collaboration, A. B. McDonald, Nucl. Phys. B (Proc. Suppl.) **91**, 21 (2000).
[23] Borexino Collaboration, G. Ranucii *et al.*, Nucl. Phys. B (Proc. Suppl.) **91**, 58 (2001).
[24] J. Busenitz *et al.*, ''Proposal for US Participation in KamLAND,'' 1999.
[25] KamLAND Collaboration, A. Piepke, Nucl. Phys. B (Proc. Suppl.) **91**, 99 (2001); V. Barger, D. Marfatia, and B. P. Wood, Phys. Lett. B **498**, 53 (2001).
[26] S. Fukuda *et al.*, Phys. Rev. Lett. **86**, 5656 (2001).